Supporting Information

MOF-derived multicomponent Fe_2P-Co_2P-Ni_2P hollow architectures for efficient hydrogen evolution

Tingjuan Wang[a], Feiran Chen[a], Jiahao Wang[a], Chao Wang[a], Long Kuai[*,b,c] Baoyou Geng[*,a,c]

[a] College of Chemistry and Materials Science, The key Laboratory of Functional Molecular Solids, Ministry of Education, The Key Laboratory of Electrochemical Clean Energy of Anhui Higher Education Institutes, Anhui Provincial Engineering Laboratory for New-Energy Vehicle Battery Energy-Storage Materials, Anhui Normal University, Wuhu, 241002, China.

[b] School of Chemical and Environmental Engineering, Anhui Polytechnic University, Wuhu, 241002, China.

[c] Institute of Energy, Hefei Comprehensive National Science Center, Anhui, Hefei, 230031, China.

Corresponding Author:

Email: bygeng@mail.ahnu.edu.cn; kuailong@ahpu.edu.cn

1. Experimental Section：

Materials. Cobalt nitrate hexahydrate ($Co(NO_3)_2·6H_2O$, Aladdin AR 99%), Nickel nitrate hexahydrate ($Ni(NO_3)_2·6H_2O$, Sinopharm Reagent Co., Ltd AR), Iron nitrate nonahydrate ($Fe(NO_3)_3·9H_2O$, Sinopharm Reagent Co., Ltd AR), 2-Methylimidazole ($C_4H_6N_2$ Macklin 98%),Sodium hypophosphite (NaH_2PO_2, Aladdin AR 99.0%), Nifion (Shanghai Yuxing Energy Technology Co., Ltd), potassium hydroxide (KOH, 99.999%, Aladdin). All chemicals were as received and not subjected to special treatment prior to use.

Synthesis of Co-MOF. First, 0.6568 g (8 m mol) of 2-methylimidazole was dissolved into 20 mL of methanol and stir for 10 min to form solution A. Then dissolve 0.582 g (2 m mol) of cobalt nitrate hexahydrate in 20 ml of methanol and stir for 10 min to form solution B. Then quickly pour solution A into solution B being stirred. After stirring for 5 minutes, take out the magneton in the beaker and stand at room temperature for 24 hours to obtain purple precipitation. After washing with anhydrous methanol for three times, put it into a vacuum oven at 60 °C for 12 h.

Synthesis of 200 μL Fe-CoNi. First, 0.04 g ferric nitrate nine hydrate was added into 5 mL of ethanol and ultrasonic for 5 min to obtain a homogeneous solution. Then weigh 50 mg of Co-MOF and dissolved it in a round bottom flask containing 30 mL of ethanol. Ultrasonic for 5 min to obtain a uniform solution. Then put the round bottom flask into an oil bath pot at 85 °C, and quickly add 0.1308 g (0.45 mmol) of nickel nitrate hexahydrate and 200 μL of iron nitrate nonahydrate solution. After stirring in an oil bath pot at 85 °C for 1 h, cool to room temperature to obtain yellow green precipitation. After washing with ethanol for three times, put it into a vacuum oven at 60 °C and dry overnight. The resulting product was named 200 μL Fe-CoNi, 50% can be obtained by the same preparation method 50 μL Fe-CoNi、1000 μL Fe-CoNi and 3000 μL Fe-CoNi material.

Synthesis of Co-Ni. Similar to the 200 μL Fe-CoNi synthesis procedure, except that ferric nitrate nonahydrate was not added during the oil bath. The obtained products were named Co-Ni-15, Co-Ni-30, Co-Ni-45 and Co-Ni-60 with different reflux times of 15min, 30min, 45min and 60min, respectively.

Synthesis of Co-Fe. The preparation procedure was similar to the synthesis procedure of 200 μL Fe-CoNi, except that nickel nitrate nonahydrate was not added during the oil bath. The obtained products were named Co-Fe-15, Co-Fe-30 and Co-Fe-45 with different reflux times of 15 min, 30 min and 45 min, respectively.

Synthesis of 200 μL Fe_2P-Co_2P-Ni_2P. The material was calcined by low-temperature phosphating in nitrogen atmosphere. Take 20 mg 200 μL Fe-CoNi sample is put into the gas outlet of tubular furnace, and 200 mg sodium hypophosphite is put into the air inlet of tubular furnace. The temperature of the tube furnace was set to 350 ^oC for 2 h, and then naturally cooled to room temperature to obtain 200 μL Fe_2P-Co_2P-Ni_2P material. The same preparation method can obtain 50 μL Fe_2P-Co_2P-Ni_2P、1000 μL Fe_2P-Co_2P-Ni_2P and 3000 μL Fe_2P-Co_2P-Ni_2P material.

Synthesis of Co-NiP. The preparation steps were the same as those for the synthesis of 200 μL Fe_2P-Co_2P-Ni_2P, and the obtained products were named Co-NiP-15, Co-NiP-30, Co-NiP-45 and Co-NiP-60, respectively.

Synthesis of Co_2P. The same as the above phosphating conditions obtained by replacing 200 μL Fe-CoNi sample with pure Co-MOF.

Material Characterizations. The morphologies and the sizes of the samples were characterized by scanning electron microscopy (SEM, Hitachi S-4800) and transmission electron microscopy (TEM, Hitachi, HT-7700). High-resolution TEM (HRTEM, FEI, Tecnai G2 F30) was used to obtain the

information on lattice fringes and high resolution mapping of materials. X-ray powder diffffraction (XRD, Bruker AXS, D8 Advance) characterizations were carried out by Cu Kα radiation. In addition, X-ray photoelectron spectroscopy (XPS, Thermo Fisher, ESCALAB 250XI) was selected to analyze the valence state with the Al Kα monochromatized radiation.

Electrocatalytic Measurements. Electrocatalytic measurements were actualized by an electrochemical workstation (Chenhua, CHI660C) with the three-electrode system in 1.0 M KOH solution at room temperature. The three-electrode system was composed of carbon rod electrode as the counter electrode, Ag/ AgCl electrode as reference electrode, and glassy carbon electrode as the working electrode. The voltages obtained from all experimental data were calibrated by the equation $E_{RHE} = E_{Ag\ /\ AgCl} + 0.059 * pH + 0.197$ V. The scanning rate of LSV curve was 5 mV/s. The LSV curves of her were IR corrected. In the point range outside the Faraday region, the double-layer capacitance (Cdl) was calculated according to the CV curves obtained at different scanning rates (40, 60, 80, 100, 120 mV/s), and the electrochemical active surface area (ESCA) had been estimated. Electrochemical impedance (EIS) tests were carried out in the frequency range from 0.01 Hz to 100 kHz at open circuit voltage. The electrochemical stability of the catalyst material was tested by cyclic voltammetry. The CV cycle range is -0.4 to -0.8 V with a scan rate of 10 mV/s. The stability test used Hg/HgO electrode as the reference electrode, and other test conditions were unchanged. The long-term stability test was carried out for 100 h at a current density of 10 $mA \cdot cm^{-2}$.

2. Additional Figures

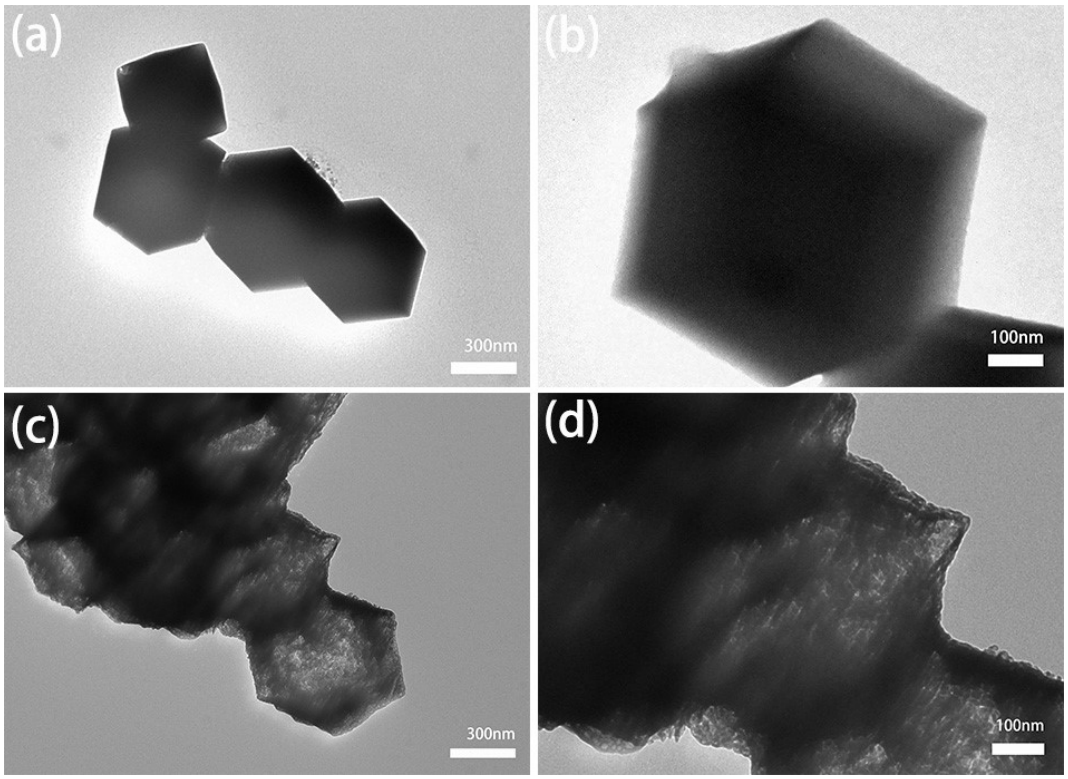

Figure S1. (a, b) Low- and high-resolution TEM images of Co-MOF. (c, d) Low- and high-resolution TEM images of Co_2P.

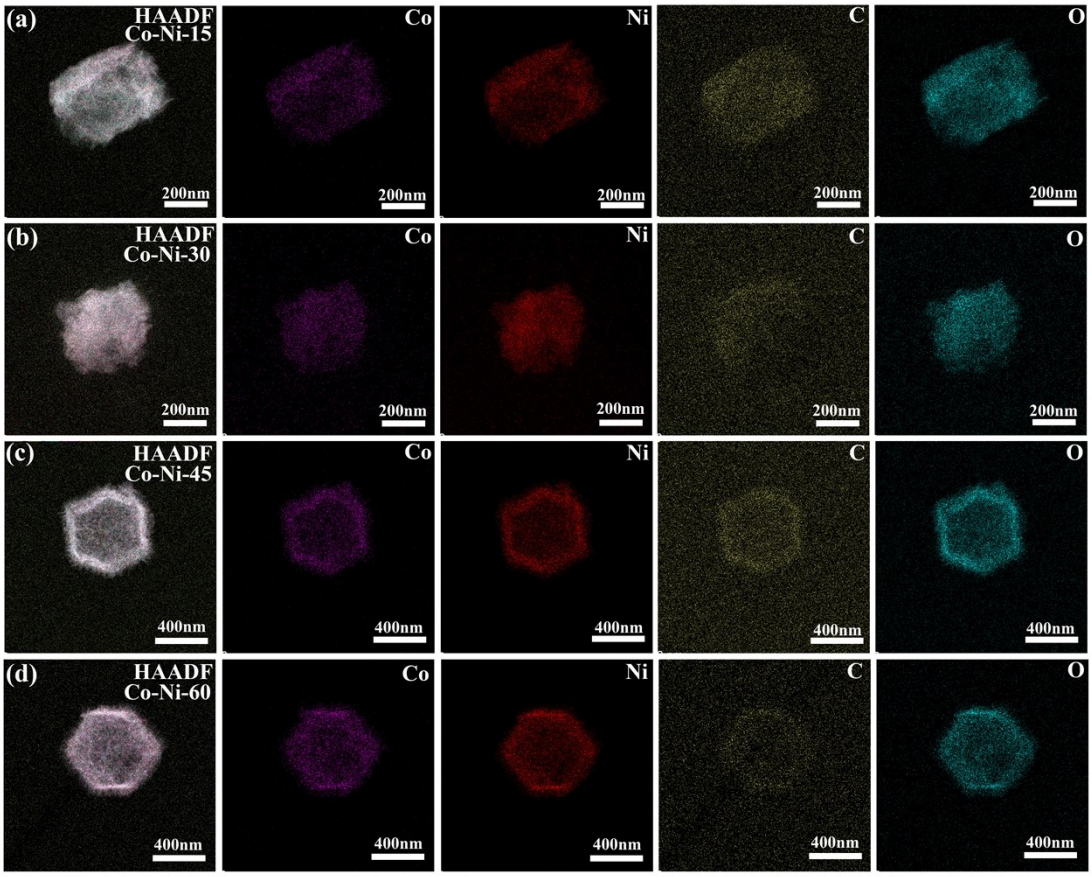

Figure S2. Mapping images of Ni^{2+} introduced into Co-MOF at different reflow times (a) Co-Ni-15, (b) Co-Ni-30, (c) Co-Ni-45, (d) Co-Ni-60.

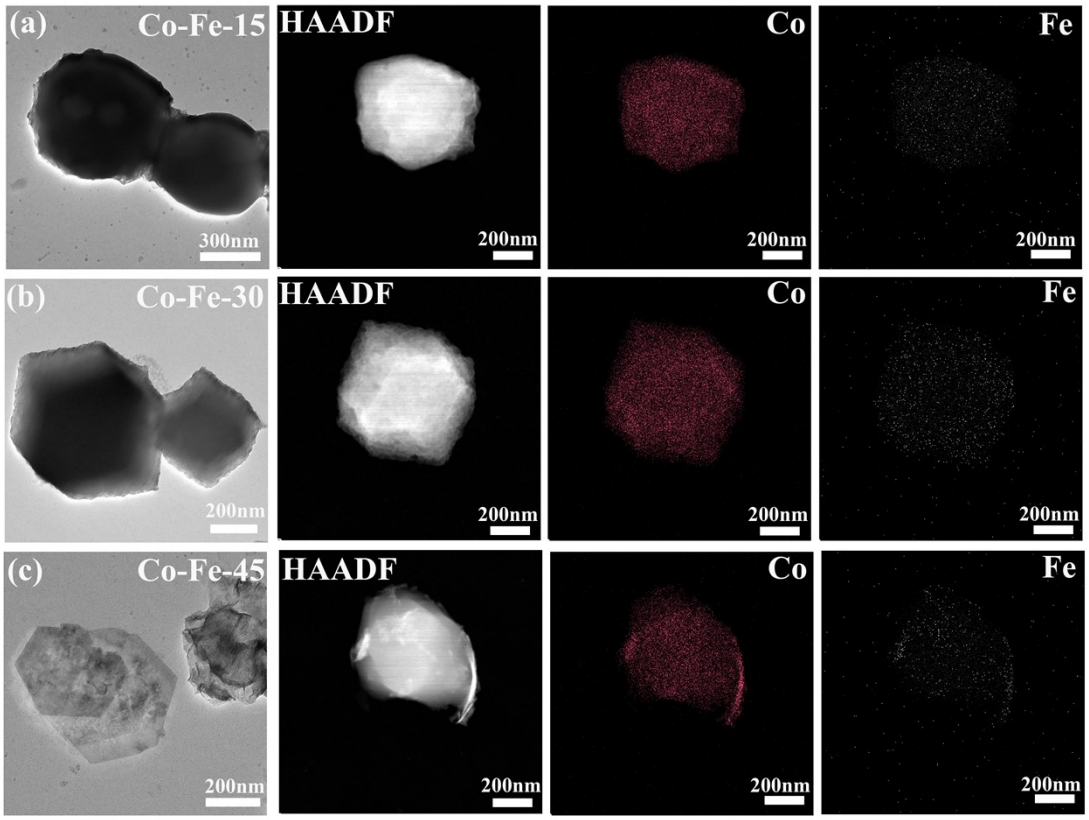

Figure S3. TEM and corresponding element transmission mapping images of Fe^{3+} introduced into Co-MOF at different reflow times (a) Co-Fe-15, (b) Co-Fe-30, (c) Co-Fe-45.

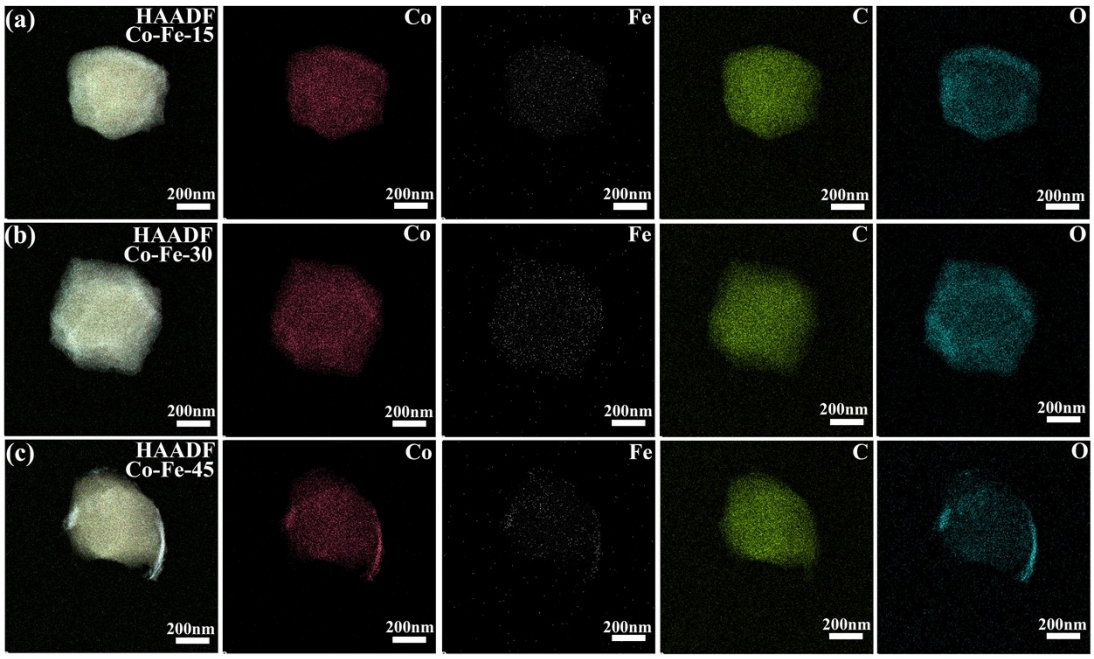

Figure S4. Mapping images of Fe^{3+} introduced into Co-MOF at different reflow times (a) Co-Fe-15, (b) Co-Fe-30, (a) Co-Fe-45.

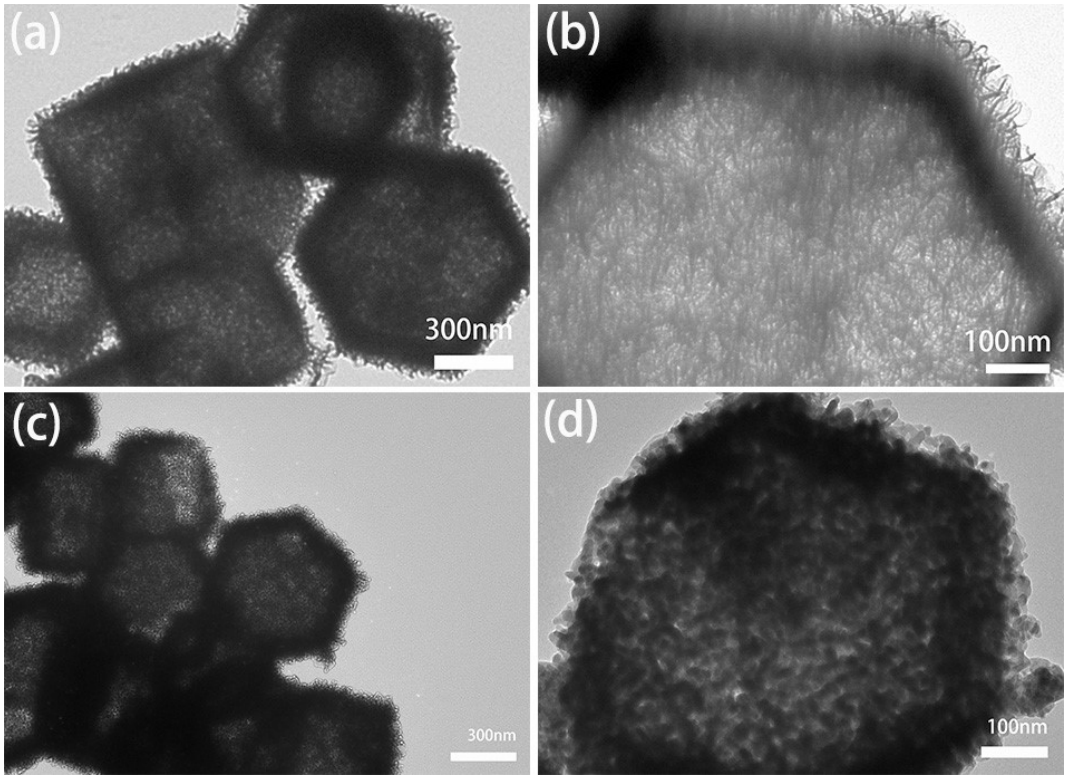

Figure S5. (a, b) Low- and high-resolution TEM images of 50 μL Fe-CoNi. (c, d) Low- and high-resolution TEM images of 50 μL Fe_2P-Co_2P-Ni_2P.

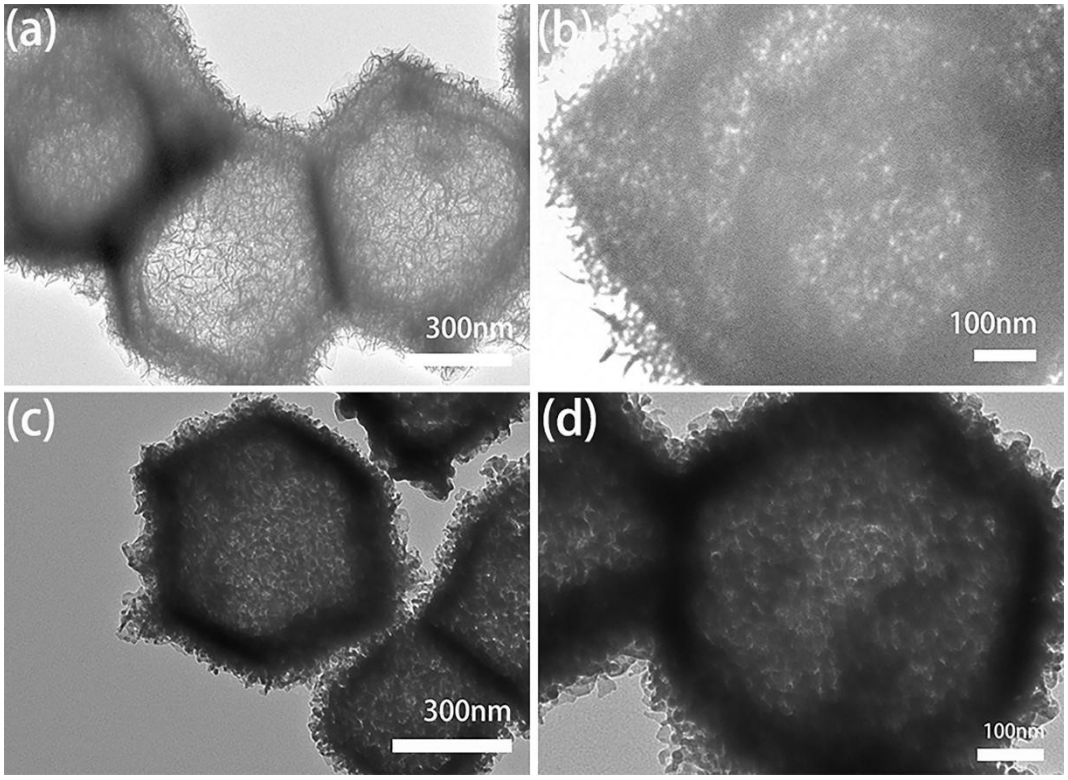

Figure S6. (a, b) Low- and high-resolution TEM images of 200 μL Fe-CoNi. (c, d) Low- and high-resolution TEM images of 200 μL Fe_2P-Co_2P-Ni_2P.

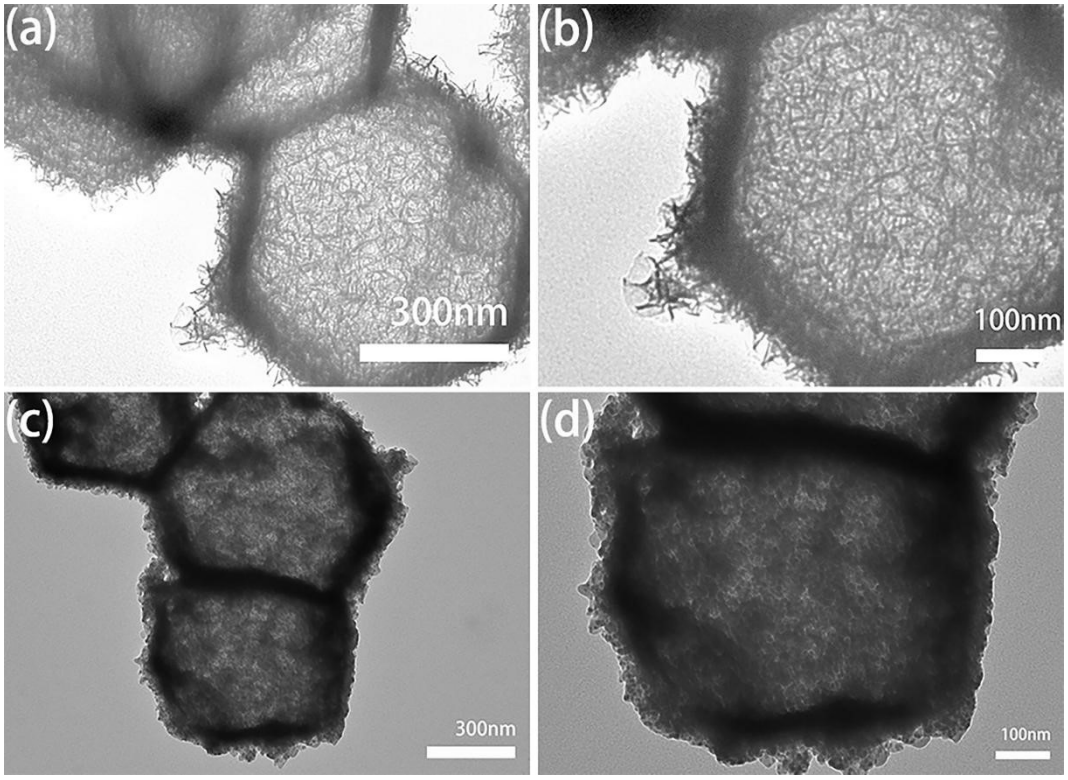

Figure S7. (a, b) Low- and high-resolution TEM images of 1000 μL Fe-CoNi. (c, d) Low- and high-resolution TEM images of 1000 μL Fe_2P-Co_2P-Ni_2P.

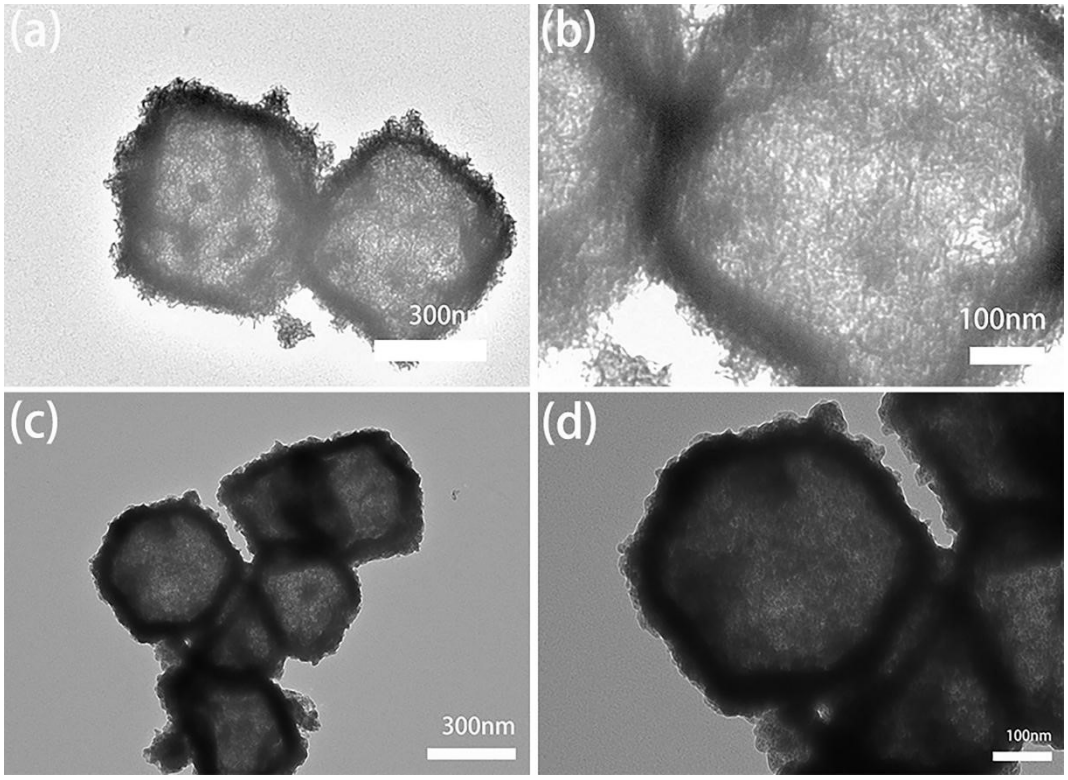

Figure S8. (a, b) Low- and high-resolution TEM images of 3000 μL Fe-CoNi. (c, d) Low- and high-resolution TEM images of 3000 μL Fe_2P-Co_2P-Ni_2P.

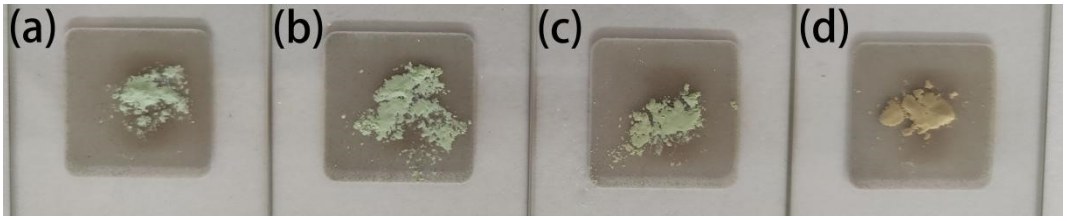

Figure S9. Photos of (a) 50 μL Fe_2P-Co_2P-Ni_2P, (b) 200 μL Fe_2P-Co_2P-Ni_2P, (c) 1000 μL Fe_2P-Co_2P-Ni_2P, (d) 3000 μL Fe_2P-Co_2P-Ni_2P.

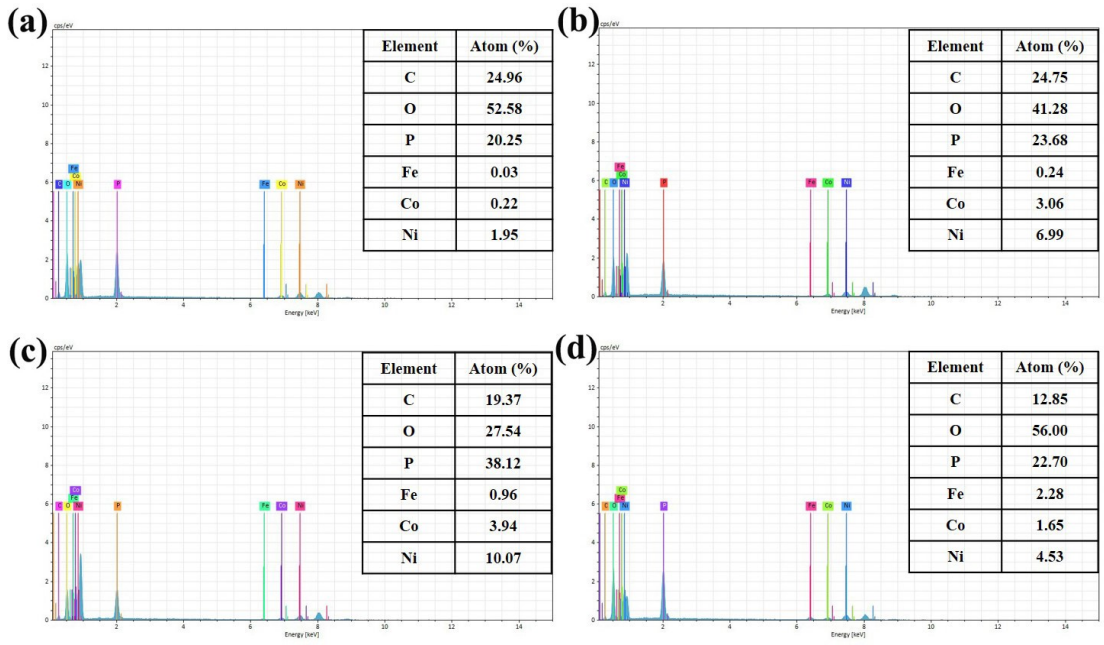

Figure S10. EDS spectra and corresponding element atomic percentage (a) 50 μL Fe_2P-Co_2P-Ni_2P, (b) 200 μL Fe_2P-Co_2P-Ni_2P, (c) 1000 μL Fe_2P-Co_2P-Ni_2P, (d) 3000 μL Fe_2P-Co_2P-Ni_2P.

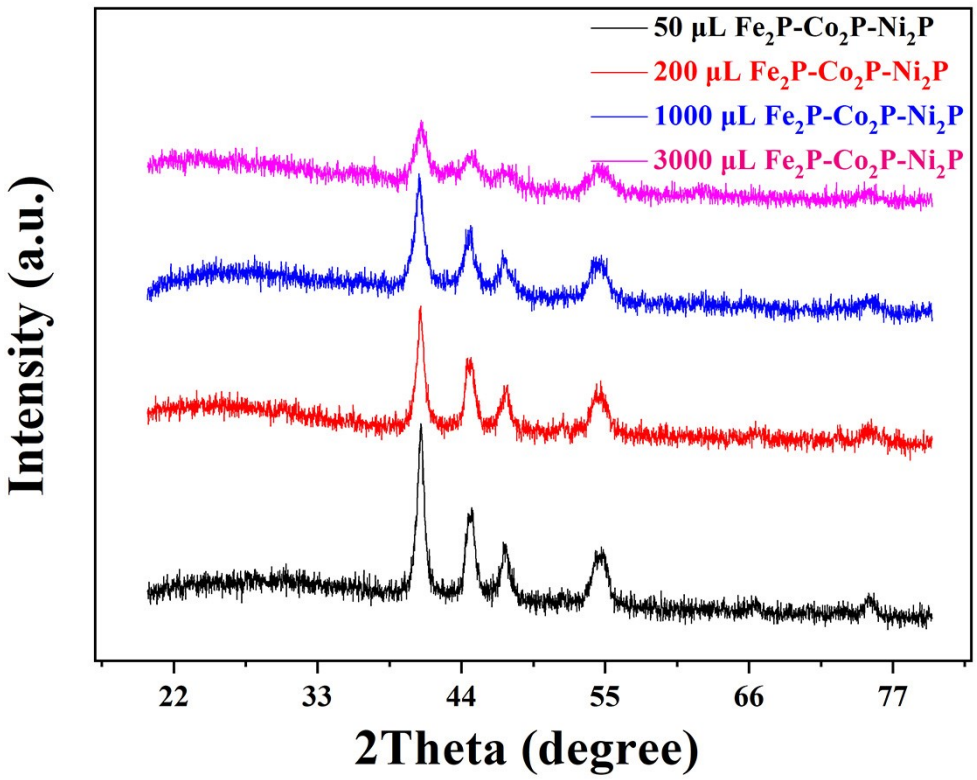

Figure S11. XRD patterns of all samples.

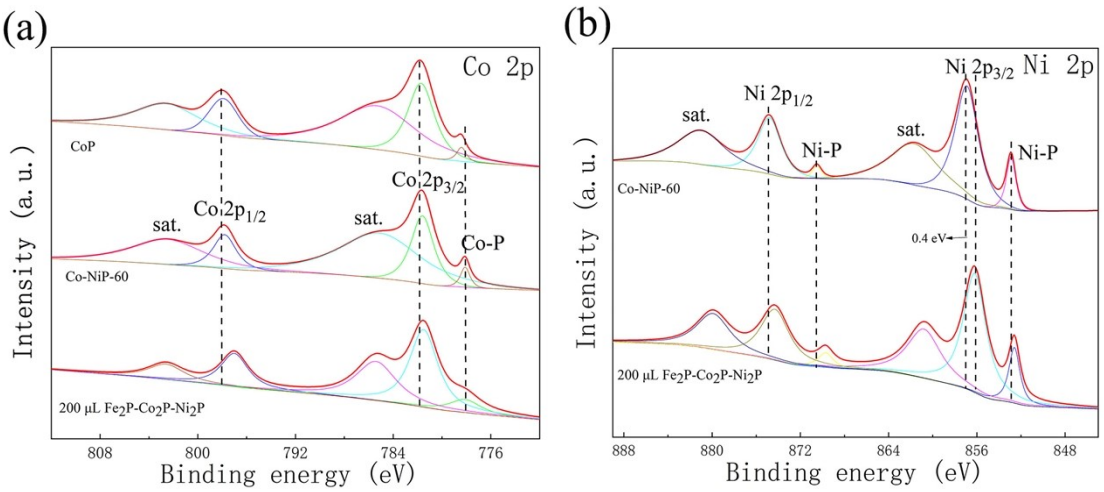

Figure S12. XPS spectra of (a) Co 2p, (b) Ni 2p performed on Co_2P, Co-NiP-60 and 200 μL Fe_2P-Co_2P-Ni_2P.

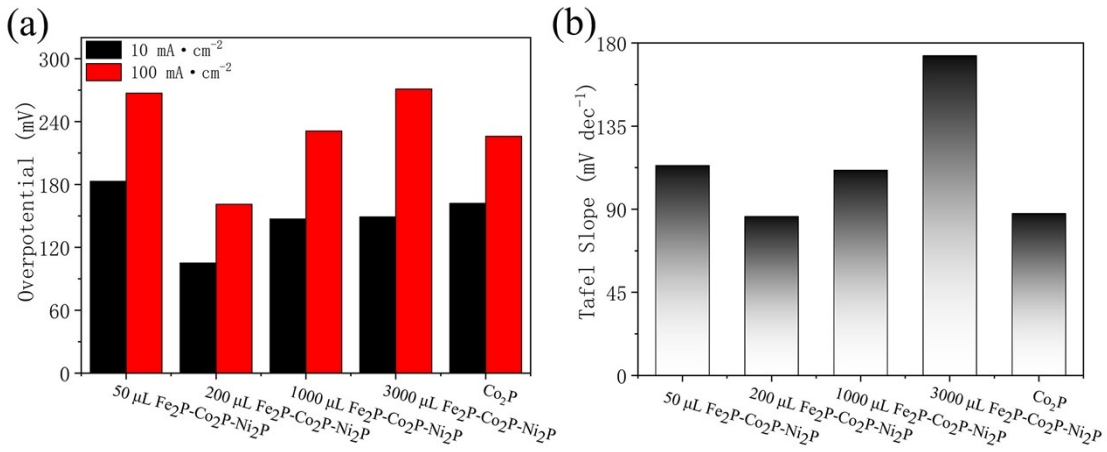

Figure S13. (a) Comparison of over potentials of catalysts at current densities of 10 mA·cm^{-2} and 100 mA·cm^{-2}. (b) Comparison of tafel slope of catalysts.

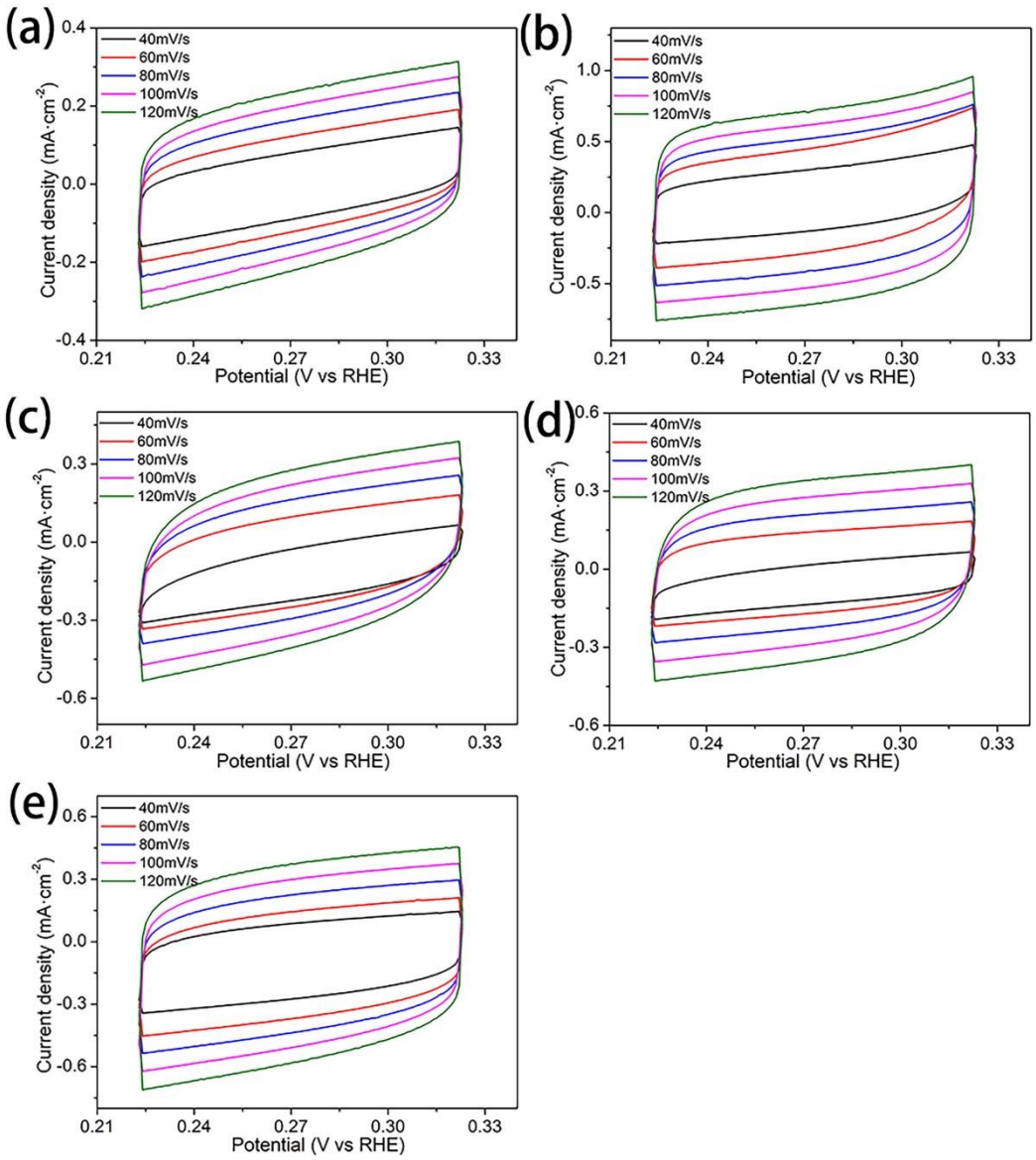

Figure S14. CV curves obtained by scanning from -0.8 v to -0.7 v (vs. RHE) at scanning speeds of 40, 60, 80, 100 and 120 mV/S (a) 50 μL Fe_2P-Co_2P-Ni_2P, (b) 200 μL Fe_2P-Co_2P-Ni_2P, (c) 1000 μL Fe_2P-Co_2P-Ni_2P, (d) 3000 μL Fe_2P-Co_2P-Ni_2P, (e) Co_2P/NF.

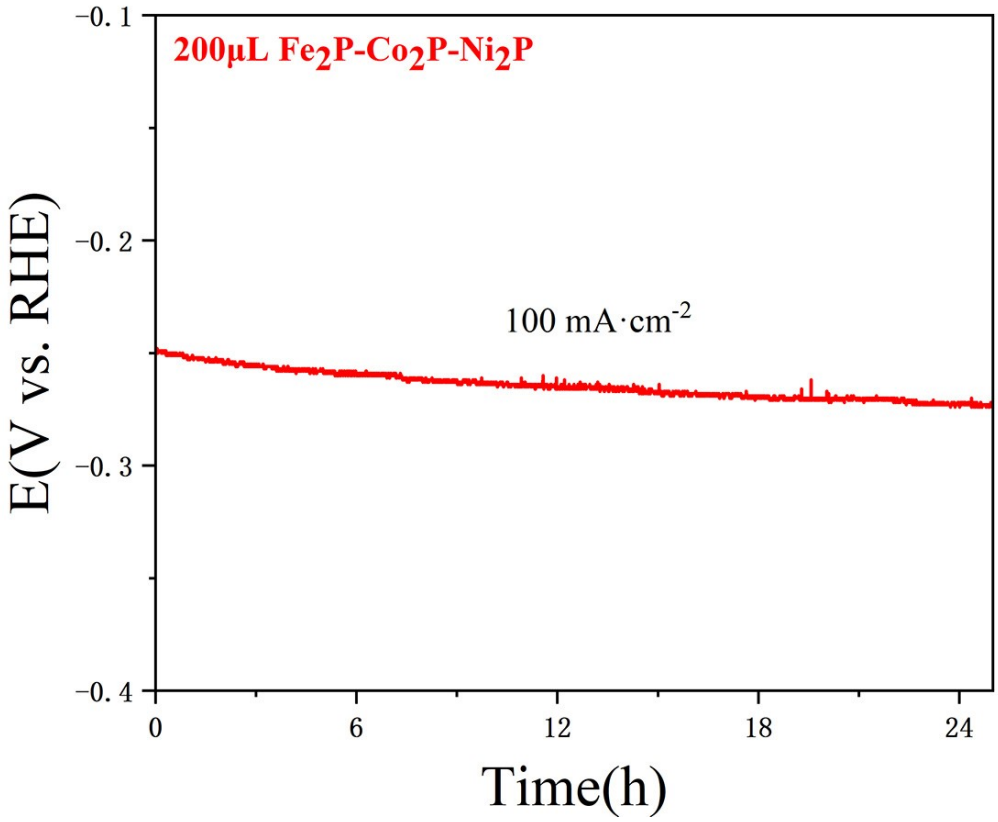

Figure S15. Chronopotentiometry curves of sample 200 μL Fe_2P-Co_2P-Ni_2P tested in 1.0 M KOH solution (IR compensation is not performed).

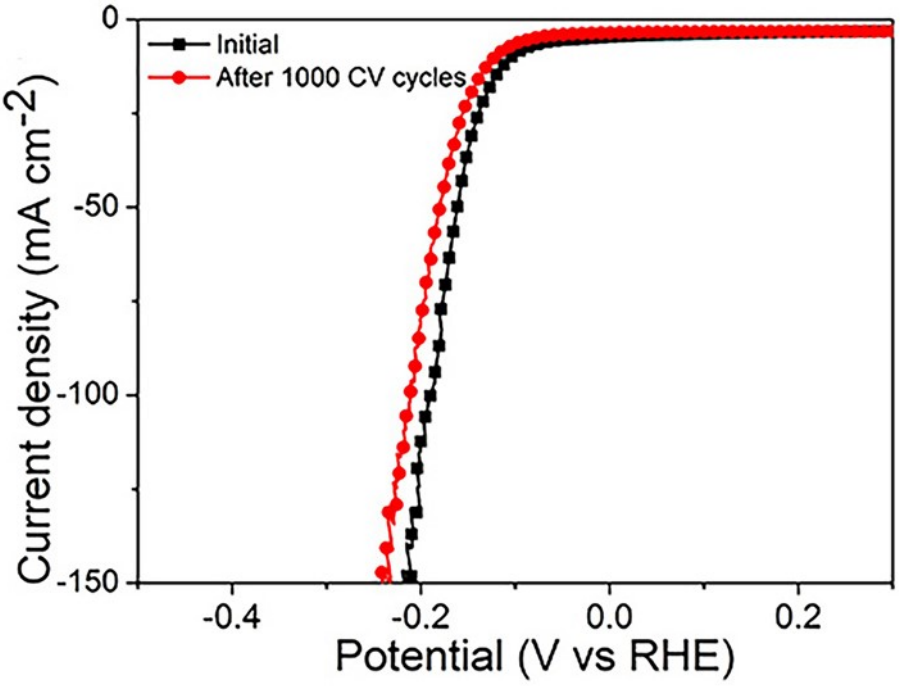

Figure S16. Polarization curves of 200 μL Fe_2P-Co_2P-Ni_2P before and after 1000 CV cycle scans.

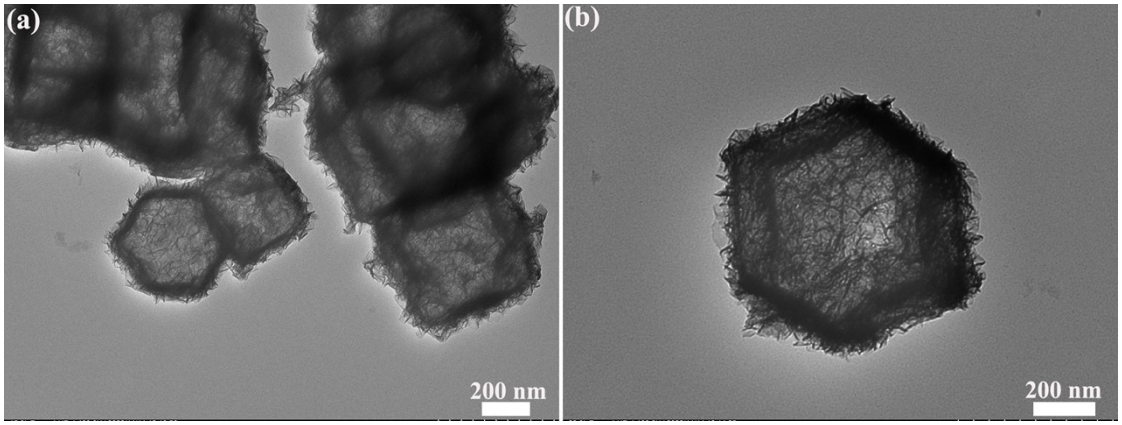

Figure S17. (a) Low- and (b) high-magnification TEM images of 200 μL Fe_2P-Co_2P-Ni_2P after 1000 CV cycles.

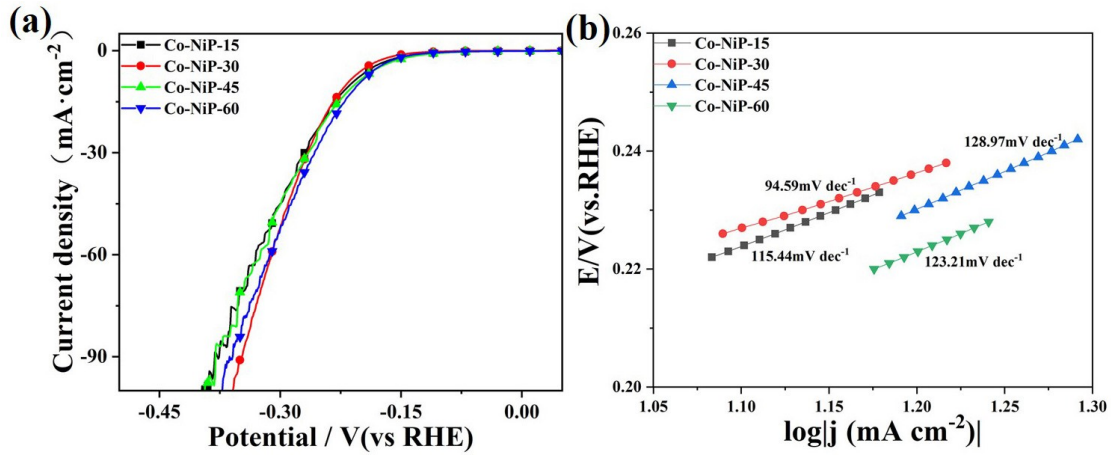

Figure S18. (a) LSV curves. (b) Tafel slope.

3. Additional Tables

Table S1. Comparison of HER activity of catalysts reported in basic (1M KOH) media with other recent catalysts.

Catalysts	η at 10 mA/cm^2 (mV)	H50 mA/cm^2 (mV)	References
Porous CoP/Co_2P nanorod	133	/	1
CoP nanoframe	136	/	2
CoFe-P/NF-1	83	~180	3
NiFeCoP/NF	/	167.5	4
CoMnP/Ni_2P/NF	108	/	5
FeP@NPC	109	/	6
MoO_2-FeP@C	103	/	7
NiO@NiP/NF	76	/	8
$(Fe_xNi_{1-x})_2P$	108	/	9
CeO_x/CoP/NF-3	117	260	10
200 μL Fe_2P-Co_2P-Ni_2P	**105**	**161**	**This work**

References

1. G. B. Liu, M. Wang, Y. S. Xu, X. Y. Wang, X. K. Li, J. Liu, X. J. Cui, L. H. Jiang, Porous CoP/Co_2P heterostructure for efficient hydrogen evolution and application in magnesium/seawater battery. Journal of Power Sources. 2021, 486, 229351.
2. L. L. Ji, J. Y. Wang, X. Teng, T. J. Meyer, Z. F. Chen, CoP Nanoframes as Bifunctional Electrocatalysts for Efficient Overall Water Splitting. ACS Catalysis. 2020, 10 (1), 412-419.
3. X. D. Wang, C. Wang, F. Y. Lai, H. X. Sun, N. Yu, B. Y. Geng, Self-Supported CoFe-P Nanosheets as a Bifunctional Catalyst for Overall Water Splitting. ACS Applied Nano

Materials. 2022, 4, 12083-12090.

4. J. M. Cen, L. Y. Wu, Y. F. Zeng, A. Ali, Y. Q. Zhu, P. K. Shen, Heterogeneous NiFeCoP/NF Nanorods as a Bifunctional Electrocatalyst for Efficient Water Electrolysis. Chemcatchem. 2021, 12, 4602-4609.
5. M. Z. Liu, Z. Sun, S. Y. Li, X. W. Nie, Y. F. Liu, E. D. Wang, Z. K. Zhao, Hierarchical superhydrophilic/superaerophobic CoMnP/Ni_2P nanosheet-based microplate arrays for enhanced overall water splitting. J. Materials Chemistry. 2021, 9, 22129-22139.
6. T. Zhang, T. X. Yang, B. Li, S. H. Wei, W. Gao, MOF-derived formation of ultrafine FeP nanoparticles confined by N/P Co-doped carbon as an efficient and stable electrocatalyst for hydrogen evolution reaction. Applied Surface Science. 2022, 597, 153662.
7. G. C. Yang, Y. Q. Jiao, H. J. Yan, Y. Xie, A. P. Wu, X. Dong, D. Z. Guo, C. G. Tian, H. G. Fu, Interfacial Engineering of MoO_2-FeP Heterojunction for Highly Efficient Hydrogen Evolution Coupled with Biomass Electrooxidation. Advanced Materials. 2020, 32 (17), 2000455.
8. C. Y. Sun, H. Wang, J. W. Ren, X. Y. Wang, R. F. Wang, Inserting ultrafine NiO nanoparticles into amorphous NiP sheets by in situ phase reconstruction for high-stability of the HER catalysts. Nanoscale. 2021, 13 (32), 13703-13708.
9. B. W. Zhang, J. J. Zhang, X. H. Tang, Y. H. Lui, S. Hu, An investigation of Fe incorporation on the activity and stability of homogeneous $(Fe_xNi_{1-x})_{(2)}$P solid solutions as electrocatalysts for alkaline hydrogen evolution. Electrochimica Acta. 2018, 294, 297-303.
10. T. Zhang, X. Wu, Y. Fan, C. Shan, B. Wang, H. Xu, Y. Tang, Hollow CeO_x/CoP Heterostructures Using Two-dimensional Co-MOF as Template for Efficient and Stable Electrocatalytic Water Splitting. ChemNanoMat. 2020, 6, 1119 -1126.